行政院國家科學委員會專題研究計畫　成果報告

豬泡疹病毒一型基因重組複合體與細胞蛋白質相互作用之研究(2/2)

計畫類別：個別型計畫
計畫編號：NSC94-2320-B-039-003-
執行期間：94 年 08 月 01 日至 95 年 07 月 31 日
執行單位：中國醫藥大學微生物學科

計畫主持人：項千芸
共同主持人：吳世祿

報告類型：完整報告

處理方式：本計畫可公開查詢

中　華　民　國 95 年 10 月 16 日

Abstract

Endonuclease G (EndoG), a member of DNA/RNA nonspecific ββα-Me-finger nucleases, is involved in mitochondrial DNA replication, apoptotic DNA fragmentation, normal cell proliferation, and herpesviral genomic inversion. To identify the critical amino acid residues of human EndoG, we replaced the conserved histidine, asparagine, and arginine residues with alanine. The catalytic efficacies of *Escherichia coli*-expressed EndoG variants were further analyzed by kinetic studies. Diethyl pyrocarbonate modification assay revealed that histidine residues were involved in EndoG activity. His-141, Asn-163, and Asn-172 in the H-N-N motif of EndoG were critical for catalysis and substrate specificity. H141A mutant required a higher magnesium concentration to achieve its activity, suggesting the unique role of His-141 in both catalysis and magnesium coordination. Furthermore, an additional catalytic residue (Asn-251) and an additional metal ion binding site (Glu-271) of human EndoG were identified. Based on the mutational analysis and homology modeling, we proposed that human EndoG shared a similar catalytic mechanism with nuclease A from *Anabaena*.

Introduction

Endonuclease G (EndoG) belongs to the large family of DNA/RNA non-specific ββα-Me-finger nucleases (1). *In vitro* studies indicated that EndoG is involved in several biological functions. For examples, EndoG is capable of processing primers for mitochondrial DNA replication (2). EndoG is also an apoptotic protein that releases from mitochondria during apoptotic process and serves as an alternative pathway to cause genomic DNA fragmentation (3-5). Moreover, EndoG initiates herpes simplex virus type 1 (HSV-1) recombination event by cleaving the HSV-1 *a* sequence (6). It is also required for normal cellular proliferation (7).

In mammals, EndoG is synthesized as a propeptide in the cytoplasm and imported into mitochondria through a process mediated by its amino-terminal mitochondrial-targeting sequences (2,8). EndoG preferentially cleaves DNA at double-stranded (dG)n·(dC)n and at single-stranded (dC)n tracts, producing 5'-phosphomonoester ends (9). The addition of EndoG to isolated nucleus first induces higher order chromatin cleavage into large DNA fragments, followed by inter- and intranucleosomal DNA cleavages (10). Although the cleavage patterns of EndoG on plasmid and chromatin have been identified, the critical amino acid residues of human EndoG remained to be clarified.

In this study, we analyzed the roles of conserved histidine, asparagine, and arginine residues in the catalysis, magnesium coordination, and substrate specificity of human EndoG. Previous study indicated that H-N-N motif of bovine EndoG is essential for catalysis (1). Herein we demonstrated that the H-N-N motif (His-141, Asn-163, Asn-172) of human EndoG was critical not only for catalysis but also for substrate specificity. His-141 was involved in magnesium coordination, suggesting the unique role of His-141 in both the catalysis and the magnesium coordination. In addition to H-N-N motif, the asparagine and glutamic acid residues near the C terminus of EndoG were identified to play a role in the catalysis and magnesium binding, respectively.

Materials and Methods

Nuclease Activity Assay - Plasmid pUC18 dsDNA, preparing with the Qiagen plasmid midi kit (Qiagen, Valencia, CA, USA), contained mainly supercoiled and a small amount of open circular DNA. For nuclease activity, 0.1 μg of pUC18 dsDNA or *Eco*RI-linearlized pUC18 dsDNA was mixed with 0.1 pmol purified human EndoG in EndoG buffer (20 mM Tris-HCl, 1 mM $MgCl_2$, 0.5 mM dithiothreitol, pH 7.5) and incubated at 37^0C for 5 min. The reaction was then stopped by the addition of stop solution (25% glycerol, 0.5% SDS, 0.05% bromophenol blue, 50 mM EDTA), and the resulting products were analyzed by electrophoresis on 1.2% agarose gels.

Chemical Modification and Hydroxylamine Restoration Assay - The chemical modification was performed as described previously (14). Briefly, EndoG (0.2 pmol) was mixed with various

amounts of diethyl pyrocarbonate (DEPC) (Sigma, St Louis, MO, USA) in 50 mM potassium phosphate buffer (pH 6.0) and incubated at 25^0C for 30 min. The reaction was then stopped by adding 100 mM imidazole (pH 6.0) to a final concentration of 1 mM. The residual activity was determined by nuclease activity assay. For hydroxylamine restoration assay, DEPC-modified EndoG was mixed with hydroxylamine to a final concentration of 20 mM and incubated at 4^0C for 5 h. The residual nuclease activity was determined under the standard assay condition. DEPC used in this study was freshly diluted with absolute ethanol, and the ethanol concentration in the reaction mixture didn't exceed 2.5% (v/v).

Site-Directed Mutagenesis - Site-directed mutagenesis was performed as described previously (14). Uracil-containing ssDNA was prepared by transforming pET-EndoG into *E. coli* CJ236 strain, which lost its deoxyuridine triphosphate nucleotidohydrolase and uracil glycosylase activities. Uracil-containing ssDNA (0.3 pmol) was annealed with 6 pmol of 5'-kinase primer in annealing buffer (20 mM Tris-HCl, 2 mM $MgCl_2$, 50 mM NaCl, pH 8.0). The second-strand DNA was then synthesized by the addition of 4 μl of 10x synthesis buffer (4 mM deoxyribonucleotides, 175 mM Tris-HCl, 37.5 mM $MgCl_2$, 5 mM dithiothreitol, 7.5 mM ATP, pH 8.0), 3 units of T4 DNA ligase and 1 unit of T4 DNA polymerase, followed by sequential incubations on ice for 5 min, at 25^0C for 5 min, and at 37^0C for 90 min. The dsDNA was then transformed into *E. coli* NM522 strain to destroy the uracil-containing strand by uracil glycosylase activity and to allow the mutated strand to be amplified. The primers for the constructions of EndoG mutants are shown in Table 1.

Kinetic Analysis - Cleavage kinetics was carried out by using various concentrations of pUC18 dsDNA substrate and constant amounts of EndoG (15). Reactions were initiated by combining reaction buffer, substrate, and enzyme in that order. Samples were mixed and incubated at 37^0C for 3 min. The products and substrates were then separated by agarose gel electrophoresis, and the intensities of products and substrates on the gel were measured by the Gel-Pro® Analyzer (Media Cybernetics, Inc., Silver Spring, MD, USA). The initial velocity was calculated by using the equation $v = \{I1/(I0+0.5I1)t\}\times[\text{substrate}]$, where t = time in seconds, I1 = product intensity, and I0 = substrate concentration. Vmax and *K*m values were calculated by directly fitting the data to the Michaelis-Menten equation, and *k*cat and *k*cat/*K*m were then derived.

Sequence-Specific Cleavage Assay - Sequence-specific cleavage assay was performed as described previously with modification (6). The plasmid DNA pKJH20, containing the HSV-1 *a* sequence, was kindly provided by Ke-Jung Huang (Department of Biochemistry, Beckman Center, Stanford University). The pKJH20 DNA was cleaved by *Eco*RI and *Xba*I to generate 2.8-kb and 1.6-kb fragments. Recombinant human EndoG was mixed with 0.2 μg of *Eco*RI/*Xba*I-treated pKJH20 in EndoG buffer containing 15 mM spermidine and incubated at 37^0C for various periods. The reactions were then stopped by the addition of stop solution, and the resulting products were analyzed by electrophoresis on 1.2% agarose gels.

Protein Structure Prediction - The structure of human EndoG was modeled using the nuclease A (NucA) from *Anabaena* (PDB code 1ZM8) as the reference protein. Protein structure was generated via the GeneSilico metaserver gateway (http://genesilico.pl/meta/) (16). 'FRankenstein's monster' approach was applied to refinement of the EndoG structure (17).

Results

Biochemical Properties of Recombinant Human EndoG - The recombinant human EndoG was purified from the *E. coli* BL21(DE3)pLysS strain transformed with a pET plasmid carrying the EndoG gene. After the induction with IPTG, EndoG was expressed in insoluble forms. The protein was then solubilized by urea and purified by nickel-affinity chromatography to homogeneity. The pH optima and cation requirements were analyzed by incubating EndoG with linear or supercoiled pUC18 dsDNA. In consistent with previous report (10), EndoG had a biphasic pH-profile with an optimum at pH 7.0 (Fig. 1*A*). The nuclease activity of EndoG was slightly stimulated when the pH value reached to pH 9.0. A sharp optimum of magnesium was obtained at 1 mM and the enzyme was inhibited at a higher magnesium concentration (4

mM)(Fig. 1*B*). Furthermore, the enzyme was activated at lower concentrations (0-5 mM) of potassium (Fig. 1*C*).

Nuclease Activity of Recombinant Human EndoG - The nuclease activity of EndoG was performed on different forms of pUC18 dsDNA. When the linear or supercoiled pUC18 dsDNA was treated with 0.01 pmol EndoG, a smear was visible after 10 min of digestion (Fig. 2*A*). When supercoiled pUC18 dsDNA was treated with EndoG, it was first converted into an open circular form. The open circular DNA was then converted to full-length linear dsDNA. With increasing EndoG concentration, the input DNA was totally degraded to low molecular weight fragments (Fig. 2*B*). These results suggested that EndoG generated single strand breaks in the plasmids, and the accumulation of nicks resulted in the double strand breaks. In conclusion, our studies on the pUC18 dsDNA substrate revealed that the catalytic properties of recombinant human EndoG were in general agreement with previous biochemical studies (6,10,18). We now focus on the previously uncharacterized catalytic center of human EndoG.

Chemical Modification of Human EndoG - Histidine residue has been implicated in the active site of several nucleases (14,19-21). In order to determine whether the histidine residue was also responsible for the catalytic activity of human EndoG, we treated EndoG with various amounts of DEPC. The residual catalytic activities of DEPC-modified EndoG were then determined under standard assay conditions. DEPC can modify different nucleophiles (such as amine, alcohol, thiols, imidazole, and guanido group), producing the carbethoxyl derivatives (22,23). At pH 6.0, DEPC is mostly specific for histidine; however, it also reacts to a smaller extent with lysine. The modified residues could be further differentiated by hydroxylamine restoration assay. Lysine-modified enzymes cannot recover their activities in the presence of hydroxylamine, whereas histidine-modified enzymes retrieve their functions after the treatment of hydroxylamine (24). Carbethoxylation of EndoG by DEPC resulted in a loss of enzyme activity, and the inactivation was dose-dependent (Fig. 3). However, treatment of DEPC-modified EndoG by hydroxylamine restored the lost catalytic activity. These findings suggested that histidine residues were involved in the catalytic activity of human EndoG.

Enzyme Kinetics of Human EndoG Variants - In addition to histidine, we also analyzed the roles of asparagine, arginine, and glutamic acid residues in EndoG activity. Asparagine and arginine are essential for catalysis in various nucleases (19,25,26). Glutamic acid has also been implicated in the magnesium binding of nucleases (27,28). By multiple alignment of EndoG homologs from human, bovine, mouse, rat, nematode, and yeast, we found that histidine residues at positions 141 and 228, asparagine residues at positions 163, 172 and 251, arginine residues at positions 110, 139, 184 and 272, and glutamic acid at position 271 of human EndoG were highly conserved (data not shown). These conserved amino acid residues were then replaced with alanine, lysine, or aspartic acid residue to generate 14 EndoG mutants. The mutants were then expressed and purified to homogeneity, and the enzyme kinetics of EndoG mutants was analyzed under Michaelis-Menten conditions.

Fig. 4 shows that the cleavage products (open circular and linear forms) were generated by EndoG. To determine the Michaelis constants (*K*m) and catalytic-centre activity (*k*cat) values of EndoG, nuclease assays were carried out using various concentrations of substrates, a constant amount of enzyme and gel electrophoresis, and the initial cleavage rates were measured by quantifying cleavage products. The *K*m and *k*cat values of wild-type EndoG derived from these experiments were 18.72±1.84 nM and 0.07±0.01 S^{-1}, respectively.

A comparison of kinetic parameters for EndoG wild type and mutants is shown in Table 2. The activities of R110A and E271A mutants could not be determined accurately, as they aggregated with supercoiled pUC18 dsDNA. Replacement of His-141 and Asn-163 with alanine and lysine, respectively, resulted in a slight decrease in *K*m. However, a dramatic reduction in *K*m was observed when the conserved arginine residues at positions 139, 184, and 272 were substituted by alanine. Mutation at Asn-251 also lead to a markedly decrease in *K*m. These findings indicated that the dissociations of the Michaelis complex between mutants (R139A,

R184A, N251A, and R272A) and DNA substrate were smaller than that of wild-type EndoG.

Mutations at His-141, Asn-163, and Asn-251 showed drastically reduced activities (<0.01%), suggesting that these amino acid residues were critical for catalysis. A large decrease in activity (~0.1%) was also observed when the asparagine at position 172 was substituted by alanine. Less dramatic effects (>10%) were observed when His-228, Arg-184, and Arg-272 were replaced with alanine. Most of the mutants were mainly affected in their *k*cat, while H141D and N251A exhibited a decrease in both *k*cat and *K*m. N172A was more affected in its *k*cat than *K*m. These findings suggested that His-141, Asn-163, Asn-172, and Asn-251 of human EndoG were involved in catalysis.

Magnesium Requirements of Human EndoG Variants - We investigated the magnesium requirements of EndoG wild type and mutants. As expected, the maximal catalytic activity of wild-type EndoG would be achieved at magnesium concentration of 1 mM (Fig. 5). Moreover, the enzyme activity of wild-type EndoG was inhibited at a higher magnesium concentration. All the EndoG mutants shared similar profiles with wild type (data not shown). However, H141A and E271A achieved the maximal activities at a 20-fold higher magnesium concentration (20 mM) than wild-type EndoG. The optimal magnesium concentration of H141A/H228A double mutant was almost the same as that of H141A. These mutants had lower affinities for the magnesium ion cofactor than the wild-type EndoG, suggesting that magnesium ion might be coordinated directly by His-141 and Glu-271 of human EndoG.

Cleavage Specificities of Human EndoG Variants - EndoG is highly specific for (dG)n·(dC)n tracts in DNA, generating single strand cleavages within the dG·dC homopolymer pair (9). We further analyzed the roles of conserved amino acid residues in the cleavage specificity of human EndoG. Sequence-specific cleavage assay was carried out by using pKJH20 as the substrate. Plasmid pKJH20 was derived from pBluescript II SK (+) by inserting a 340-bp HSV-1 *a* sequence-containing fragment into the *Bam*HI site and a 1.24-kb kanamycin cassette into the *Pst*I site. The *a* sequence is a GC-rich (85%) fragment, containing many strings of dGn (n=4-8) (6). Plasmid pKJH20 was cleaved by *Eco*RI and *Xba*I to generate the 2.8-kb and 1.6-kb substrates, where the GC-rich fragment is located within the 1.6-kb fragment (Fig. 6*A*). When the enzyme cleaved DNA within the GC-rich fragment, the 1.6-kb substrate fragment would be cleaved to generate the 1.3-kb product fragment. As shown in Fig. 6*B*, wild-type EndoG initially cleaved the 1.6-kb fragment to generate the 1.3-kb fragment. With prolonging the digestion time, EndoG cleaved both fragments (2.8 kb and 1.6 kb) to generate diffuse bands. Mutations at arginine residues displayed the similar cleavage patterns with wild type. R110A, R139A, and R184A preferentially cleaved the 1.6-kb fragment. When the incubation period was extended, the 1.6-kb fragment was totally digested to generate the 1.3-kb fragment, and both fragments (2.8 kb and 1.3 kb) were consequently degraded to generate diffuse bands. In contrast to these mutants, H141A, N163A, N172A, and N251A cleaved both fragments equally. With extending the digestion time, both fragments were degraded to low-molecular-weight-fragments. These findings suggested that His-141, Asn-163, Asn-172, and Asn-251 were critical for substrate specificity, while Arg-110, Arg-139, and Arg-184 might not be involved in the cleavage specificity.

Discussion

In this study, we demonstrated the roles of conserved histidine, arginine, and asparagine residues in catalysis, magnesium coordination, and substrate specificity of human EndoG. The primary sequence analysis revealed that EndoG contained the DRGH prosite motif, which is a characteristic of highly active, divalent metal ion-dependent, non-specific nucleases (Fig. 7*A*) (28). The site-directed mutagenesis analysis demonstrated that H-N-N motif (His-141, Asn-163, and Asn-172) of human EndoG were critical for catalysis and substrate specificity. The secondary structure analysis revealed that EndoG contained an active site with the ββα-Me-finger fold, which is the characteristic of many H-N-H superfamily endonucleases (Fig. 7*A*) (26). Based on the results of our analysis, we reported herein the biochemical evidence for human EndoG that

belongs to the H-N-H superfamily and exhibits a catalytic motif based on the ββα-Me-finger fold.

The H-N-H nucleases include heterogeneous group of enzymes with diverse functions but with similar active sites. A few examples are: sugar nonspecific nucleases such as NucA and *Serratia* nuclease (28,29), nonspecific DNases such as *E. coli* colicin E9 (ColE9) (30), homing endonucleases such as I-*Ppo*I (31), structure-specific nucleases such as T4 endonuclease VII (T4endoVII) (32), and type II restriction endonucleases such as *Kpn*I (21). A similar ββα-Me topology has been revealed in the active site regions of these nucleases (33). Moreover, the H-N-H motif, characterized by the presence of a conserved Asn/His residue flanked by conserved His and His/Asn residues at some distance, is presented in these endonucleases (29-31). The histidine residue in the ββα-Me finger is ideally positioned to act as a general base to activate a water molecule for the nucleophilic attack on the phosphorous atom (28). By results of mutational analysis, we revealed that His-141 was responsible for catalysis of human EndoG. His-141 was also highly conserved among these nucleases (NucA, His-124; *Serratia* nuclease, His-89; ColE9, His-103; I-*Ppo*I, His-98; T4endoVII, His-41) (19,30,34-36). These findings indicated that His-141 of human EndoG would act as a general base.

Magnesium, the most abundant divalent metal ion in mammalian cells, plays structural and catalytic roles in many cellular processes (37). Magnesium ion functions as a cofactor of proteins involved in DNA replication and repair pathways (38). It is required for activity and fidelity of DNA polymerase (39). It is also required for the activities of nucleases, such as apurinic/apyrimidinic endonuclease, MutH, RNase A, DNase I, and viral DNase (12,40-43). The active site of the H-N-H endonucleases supplies one or two magnesium ligands as identified by crystal structure analysis: Asn-155 in NucA, Asn-119 in *Serratia* nuclease, His-102 and His-127 in ColE9, Asn-119 in I-*Ppo*I, Asp-40 and Asn-62 in T4endoVII (28-30,32,35). Traditionally, enzymes that utilize magnesium are known to contain metal-binding sites that are created by acidic residues (44-46). However, there is precedent for the binding of magnesium by histidine in several enzymes. For examples, His-607 and His-643 of phosphodiesterase-5 act as direct participants in coordinating the magnesium required for catalysis (47). His-102 and His-127 of ColE9 are included in the coordination shell of a magnesium ion in the colicin E9 active site (30). Previous study suggested that Asn-174 of bovine EndoG, corresponding to Asn-172 of human EndoG, is a putative magnesium ligand (1). By results of mutagenesis, we demonstrated that His-141 instead of Asn-172 might be coordinated with magnesium because H141A mutant required a higher magnesium concentration to achieve the maximal activity. These findings suggested the unique role of His-141 in both catalysis and magnesium binding of human EndoG. In addition to His-141, an additional residue (Glu-271) located near the C terminus of human EndoG was also coordinated with magnesium ion. A second metal binding site (glutamic acid) located near the C terminus of the protein was present in human EndoG (Glu-271) and Nuc (Glu-249) but not in other H-N-H endonucleases (28). These findings suggested the closest similarity between EndoG and NucA.

Human EndoG participates in the HSV-1 genomic inversion by cleaving the *a* sequence (6). The recombinant human EndoG preferentially cleaved the GC-rich fragment, also indicating that EndoG preferentially cleaved at the GC-rich sequence. However, the sequence preferences of EndoG mutants were disappeared; H141A, N163A, N172A, and N251A cleaved both fragments to generate low-molecular-weight fragments. These results suggested that His-141, Asn-163, Asn-172, and Asn-251 were required not only for catalysis but also for sequence specificity of human EndoG. Previous study proposed that arginine residues are critical for DNA binding of bovine EndoG (1). However, the cleavage specificities of R110A, R139A, and R184A were similar as that of wild type. These results suggested that arginine residues at positions 110, 139, and 184 of human EndoG might be involved in the DNA substrate interactions but not in the cleavage site determination.

Mutational analysis indicated that H-N-N motif (His-141, Asn-163, Asn-172) of human EndoG was essential for catalysis. N251A mutant lost its enzyme activity, indicating that Asn-251 was also involved in catalysis. Moreover, His-141 and Glu-271 were critical for magnesium coordination. Since the H-N-H motif, Asn-251 residue, and Glu-271 residue were highly conserved in human EndoG and NucA, we build a homology model of the three-dimentional

structure of human EndoG based on the crystal structure of NucA (Fig. 7*B*). A good structural superposition for human EndoG and NucA could be achieved. Three arginine residues, Arg-110, Arg-139, and Arg-184, were distributed on a line. A rigid V-shaped architecture of human EndoG formed the catalytic site, where His-141, Asn-163, and Asn-172 were located within the cleft. Based on the mutational analysis and homology modeling, we proposed that the V-shaped cleft of human EndoG might be involved in DNA cleavage, DNA binding, and substrate recognition. It is noticed that an additional catalytic residue, Asn-251, and the additional magnesium coordinated site, Glu-271, were potentially located far from the cleft. How the Asn-251 and Glu-271 cooperated with H-N-N motif and participated in the DNA catalysis remained to be further clarified.

In conclusion, the roles of conserved histidine, arginine, and asparagine residues in catalytic, magnesium coordination, and substrate specificity of human EndoG were analyzed. The H-N-N motif (His-141, Asn-163, Asn-172) of human EndoG was critical for catalysis and substrate specificity. His-141 was also essential for magnesium coordination. An additional catalytic residue (Asn-251) and an additional magnesium ligand (Glu-271) of human EndoG were identified. Based on the mutational analysis and homology modeling, we speculated that human EndoG shared a similar catalytic mechanism with nuclease A from *Anabaena*.

References

1. Schäfer, P., Scholz, S. R., Gimadutdinow, O., Cymerman, I. A., Bujnicki, J. M., Ruiz-Carrillo, A., Pingoud, A., and Meiss, G. (2004) *J. Mol. Biol.* **338,** 217-228
2. Cote, J., and Ruiz-Carrillo, A. (1993) *Science* **261,** 765-769
3. Li, L. Y., Luo, X., and Wang, X. (2001) *Nature* **412,** 95-99
4. Parrish, J., Li, L., Klotz, K., Ledwich, D., Wang, X., and Xue, D. (2001) *Nature* **412,** 90-94
5. van Loo, G., Schotte, P., van Gurp, M., Demol, H., Hoorelbeke, B., Gevaert, K., Rodriguez, I., Ruiz-Carrillo, A., Vandekerckhove, J., Declercq, W., Beyaert, R., and Vandenabeele, P. (2001) *Cell Death Differ.* **8**, 1136-1142
6. Huang, K. J., Zemelman, B. V., and Lehman, I. R. (2002) J. Biol. Chem. 277, 21071-21079
7. Huang, K. J., Ku, C. C., and Lehman, I. R. (2006) *Proc. Natl. Acad. Sci. USA* **103,** 8995-9000
8. Gerschenson, M., Houmiel, K. L., and Low, R. L. (1995) *Nucleic Acids Res.* **23,** 88-97
9. Ruiz-Carrillo, A., and Renaud, J. (1987) *EMBO J.* **6,** 401-407
10. Widlak, P., Li, L. Y., Wang, X., and Garrard, W. T. (2001) *J. Biol. Chem.* **276,** 48404-48409
11. Chomczynski, P., and Sacchi, N. (1987) *Anal. Biochem.* **162,** 156-159
12. Hsiang, C. Y., Ho, T. Y., Hsiang, C. H., and Chang, T. J. (1998) *Biochem. J.* **330,** 55-59
13. Wu, S. L., Hsiang, C. Y., Ho, T. Y., and Chang, T. J. (1998) *Virus Res.* **56,** 1-9
14. Ho, T. Y., Wu, S. L., Hsiang, C. H., Chang, T. J., and Hsiang, C. Y. (2000) *Biochem. J.* **346,** 441-445
15. Qiu, J., Bimston, D. N., Partikian, A., and Shen, B. (2002) *J. Biol. Chem.* **277,** 24659-24666
16. Kurowski, M. A., and Bujnicki, J. M. (2003) *Nucleic Acids Res.* **31,** 3305-3307
17. Kosinski, J., Cymerman, I. A., Feder, M., Kurowski, M. A., Sasin, J. M., and Bujnicki, J. M. (2003) *Proteins* **53,** 369-379
18. Ohsato, T., Ishihara, N., Muta, T., Umeda, S., Ikeda, S., Mihara, K., Hamasaki, N., and Kang, D. (2002) *Eur. J. Biochem.* **269,** 5765-5770
19. Friedhoff, P., Kolmes, B., Gimadutdinow, O., Wende, W., Krause, K. L., and Pingoud, A. (1996) *Nucleic Acids Res.* **24,** 2632-2639
20. Walker, D. C., Georgiou, T., Pommer, A., Walker, D., Moore, G. R., Kleanthous, C., and James, R. (2002) *Nucleic Acids Res.* **30,** 3225-3234
21. Saravanan, M., Bujnicki, J. M., Cymerman, I. A., Rao, D. N., and Nagaraja, V. (2004) *Nucleic Acids Res.* **32,** 6129-6135
22. Melchior, Jr, W. B., and Fahrney, D. (1970) *Biochemistry* **9,** 251-258
23. Dominici, P., Tancini, B., and Voltattorni, C. B. (1985) *J. Biol. Chem.* **260,** 10583-10589
24. Burstein, Y., Walsh, K. A., and Neurath, H. (1974) *Biochemistry* **13,** 205-210

25. Garinot-Schneider, C., Pommer, A. J., Moore, G. R., Kleanthous, C., and James, R. (1996) *J. Mol. Biol.* **260,** 731-742
26. Scholz, S. R., Korn, C., Bujnicki, J. M., Gimadutdinow, O., Pingoud, A., and Meiss, G. (2003) *Biochemistry* **42,** 9288-9294
27. Sun, W., and Nicholson, A.W. (2001) *Biochemistry* **40,** 5102-5110
28. Ghosh, M., Meiss, G., Pingoud, A., London, R. E., and Pedersen, L. C. (2005) *J. Biol. Chem.* **280,** 27990-27997.
29. Miller, M. D., Cai, J., and Krause, K. L. (1999) *J. Mol. Biol.* **288,** 975-987
30. Maté, M. J., and Kleanthous, C. (2004) *J. Biol. Chem.* **279,** 34763-34769.
31. Kowalski, J. C., and Derbyshire, V. (2002) *Methods* **28,** 356-373
32. Raaijmarkers, H., Toro, I., Birkenbihl, R., Kemper, B., and Suck, D. (2001) *J. Mol. Biol.* **308,** 311-323
33. Kühlmann, U. C., Moore, G. R., James, R., Kleanthous, C., and Hemmings, A. M. (1999) *FEBS Lett.* **463,** 1-2.
34. Golza, S., Christoph, A., Birkenkamp-Demtroder, K., and Kemper, B. (1997) *Eur. J. Biochem.* **245,** 573-580
35. Garlburt, E. A., Chevalier, B., Tang, W., Jurica, M. S., Flick, K. E., Monnat, R. J., Jr., and Stoddard, B. L. (1999) *Nat. Struct. Biol.* **6,** 1096-1099
36. Meiss, G., Gimadutdinow, O., Haberland, B., and Pingoud, A. (2000) *J. Mol. Biol.* **297,** 521-534
37. Hartwig, A. (2001) *Mutat. Res.* **475,** 113-121.
38. Barzilay, G., Mol, C. D., Robson, C. N., Walker, L. J., Cunningham, R. P., Tainer, J. A., and Hickson, I. D. (1995) *Nat. Struct. Biol.* **2,** 561-568.
39. Sirover, M. A., and Loeb, L. A. (1977) *J. Biol. Chem.* **252,** 3605-3610
40. Takahashi, T., Irie, M., and Ukita, T. (1967) *J. Biochem. (Tokyo)* **61,** 669-678
41. Baril, E., Mitchener, J., Lee, L., and Baril, B. (1977) *Nucleic Acids Res.* **4,** 2641-2653
42. Welsh, K. M., Lu, A. L., Clark, S., and Modrich, P. (1987) *J. Biol. Chem.* **262,** 15624-15629
43. Wilson, D. M. 3rd. (2005) *J. Mol. Biol.* **345,** 1003-1014
44. Hough, E., Hansen, L. K., Birknes, B., Jynge, K., Hansen, S., Hordvik, A., Little, C., Dodson, E., and Derewenda, Z. (1989) *Nature* **338,** 357-360
45. Beese, L. S., and Steitz, T. A. (1991) *EMBO J.* **10,** 25-33
46. Murphy, J. E., Xu, X., and Kantrowitz, E. R. (1993) J. Biol. Chem. **268,** 21497-21500
47. Francis, S. H., Turko, I. V., Grimes, K. A., and Corbin, J. D. (2000) *Biochemistry* **39,** 9591-9596
48. Tiranti, V., Rossi, E., Ruiz-Carrillo, A., Rossi, G., Rocchi, M., DiDonato, S., Zuffardi, O., and Zeviani, M. (1995) *Genomics* **25,** 559-564
49. Muro-Pastor, A. M., Flores, E., Herrero, A., and Wolk, C. P. (1992) *Mol. Microbiol.* **6,** 3021-3030
50. Ball, T. K., Saurugger, P. N., and Benedik, M. J. (1987) *Gene* **57,** 183-192
51. Lau, P. C., and Condie, J. A. (1989) *Mol. Gen. Genet.* **217,** 269-277
52. Muscarella, D. E., Ellison, E. L., Ruoff, B. M., and Vogt, V. M. (1990) *Mol. Cell. Biol.* **10,** 3386-3396
53. Tomaschewski, J., and Ruger, W. (1987) *Nucleic Acids Res.* **15,** 3632-3633

Table I
DNA oligonucleotides for the constructions of human EndoG mutants

Primer name	Primer sequence[a]
R110A	5′-GCACTCTCGAGCGTCGCCGTCGCCGCGGAGACG-3′
R139A	5′-CAGGTGGCCGGCGTCGAAGCCACTGCCGCGG-3′
H141A	5′-GGCCAGGGCCCCGCGGTCGAAGCCACTGCC-3′
H141D	5′-GGCCAGATCTCCGCGGTCGAAGCCACTGCCGC-3′
N163A	5′-GGGGCGCTACAGCGCTCAGGTAGAACGTGTCGTCC-3′
N163K	5′-CACCTGGGGCGCGACCTTGCTCAGGTAGAAC-3′
N172A	5′-CATTCTGCGCAAGGTGGGGCACCTGGGGCGCG-3′
R184A	5′-TCAAGCTTGCGCTATATTTCTCCAGGTTGTTCC-3′
H228A	5′-TTGAAGAATGCTGTGGGCACTGCCACGTGG-3′
H228D	5′-GAAGAAGTCTGTAGGCACTGCCACGTGGTTCTTGCC-3′
N251A	5′-AGGTGCTGCAGGCATCACGTAGGTGCGGAGC-3′
E271A	5′-CGAAGCCCGAGCAATGCTCTCGATGGGCACCAGG-3′
R272A	5′-CAGCCCTGAGGCCGCCTCAATGCTCTCGATGGGCACC-3′

[a] Boxed sequences indicate codon changes

Table II
Steady-state kinetic data for human EndoG variants

EndoG variants	*K*m (nM)*	*k*cat (S^{-1})*	*k*cat/*K*m ($S \cdot nM^{-1}$)*
Wild type	18.72±1.84	0.07±0.01	$3.58x10^{-3}$±$3.11x10^{-4}$
R110A	n.d.	n.d.	n.d.
R139A	1.01±0.03	$2.77x10^{-5}$±$4.44x10^{-7}$	$2.75x10^{-5}$±$1.47x10^{-6}$
H141A	12.93±2.17	$2.48x10^{-6}$±$4.34x10^{-7}$	$1.96x10^{-7}$±$4.78x10^{-8}$
H141D	1.94±0.05	$9.68x10^{-6}$±$2.59x10^{-13}$	$5.03x10^{-6}$±$1.72x10^{-7}$
N163A	8.51±2.28	$7.52x10^{-6}$±$1.41x10^{-6}$	$9.05x10^{-7}$±$7.67x10^{-8}$
N163K	12.10±2.03	$2.35x10^{-6}$±$1.85x10^{-7}$	$1.99x10^{-7}$±$1.61x10^{-8}$
N172A	8.75±0.13	$3.77x10^{-5}$±$4.26x10^{-8}$	$4.31x10^{-6}$±$5.95x10^{-8}$
R184A	1.53±0.02	$7.68x10^{-3}$±$3.27x10^{-10}$	$5.03x10^{-4}$±$1.91x10^{-5}$
H228A	6.01±1.88	$5.34x10^{-3}$±$2.71x10^{-3}$	$8.61x10^{-4}$±$1.81x10^{-4}$
H228D	5.70±0.33	$4.74x10^{-4}$±$1.78x10^{-5}$	$8.33x10^{-5}$±$1.75x10^{-6}$
N251A	3.13±0.37	$3.15x10^{-6}$±$5.68x10^{-14}$	$1.02x10^{-6}$±$6.64x10^{-8}$
E271A	n.d.	n.d.	n.d.
R272A	2.30±0.20	$3.67x10^{-3}$±$9.23x10^{-5}$	$1.61x10^{-3}$±$9.96x10^{-5}$
H141A/H228A	8.06±1.92	$1.18x10^{-7}$±$1.26x10^{-8}$	$1.48x10^{-8}$±$1.98x10^{-9}$

* Data are presented as mean ± standard error of triplicate assays.
n.d. , not determined.

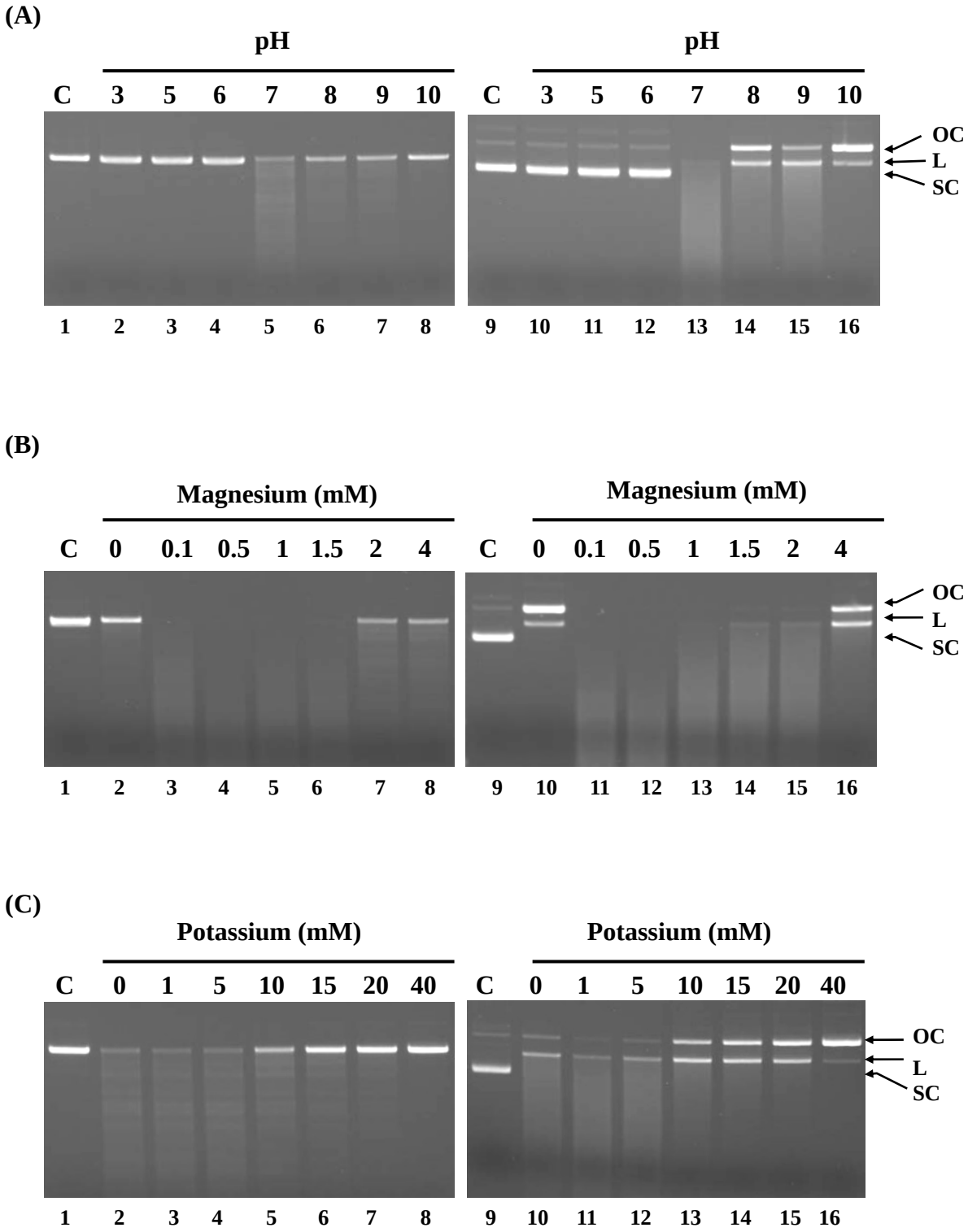

Fig. 1. Effects of pH and cation on the nuclease activity of recombinant human EndoG. The reaction mixtures containing 0.1 pmol mature EndoG and 0.1 μg pUC18 dsDNA were incubated at 37^0C for 2 min. The resulting products were then analyzed by 1.2% agarose gels. *A*, pH effect. The following buffers were used to construct the pH curve: BES (pH 3.0), acetic acid (pH 5.0), sodium phosphate (pH 6.0), Tris-HCl (pH 7 to 9), and CHAPS (pH 10). *B*, Magnesium effect. *C*, Potassium effect. *Lane C* represents the reaction performed in the absence of EndoG. *Lanes 1* to *8* represent the reactions carried out with linear pUC18 dsDNA. *Lanes 9* to *16* represent the reactions performed with supercoiled pUC18 dsDNA. *Arrowheads* denote the different topological forms of pUC18 plasmids. OC: open circular; L: linear; SC: supercoiled.

(A)

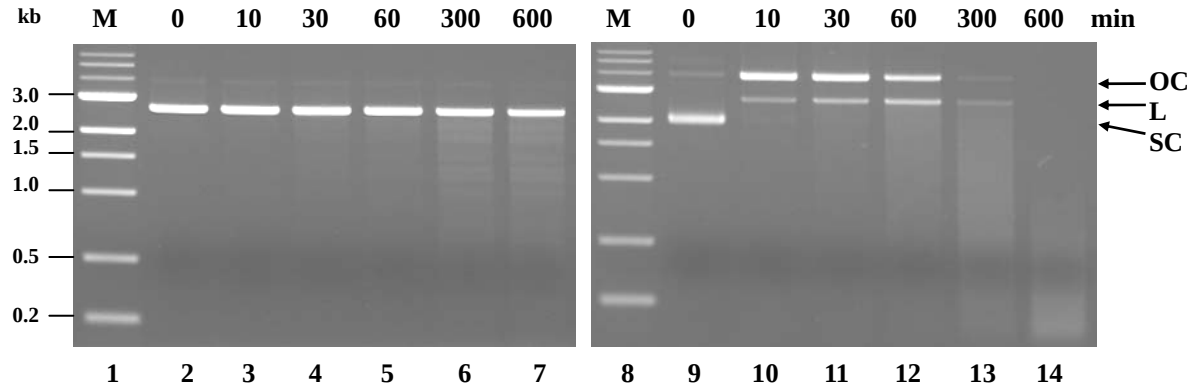

(B)

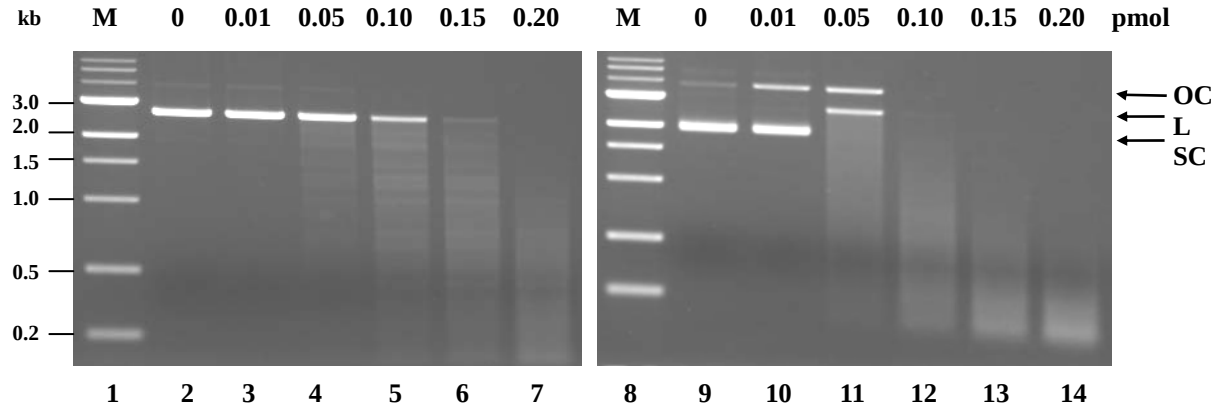

Fig. 2. Nuclease activity of recombinant human EndoG. *A*, Time course. The reaction mixtures containing 0.01 pmol EndoG and 0.1 μg pUC18 dsDNA were incubated at 37^0C for indicated periods. *B*, Dose response. The reaction mixtures containing 0.1 μg pUC18 dsDNA and various amounts of EndoG were incubated at 37^0C for 2 min. The resulting products were then analyzed by 1.2% agarose gels. *Lane M* represents the DNA standards. *Lanes 2* to *7* and *lanes 9* to *14* represent the reactions carried out with linear pUC18 dsDNA and supercoiled pUC18 dsDNA, respectively. *Arrowheads* denote the different topological forms of pUC18 plasmids. OC: open circular; L: linear; SC: supercoiled.

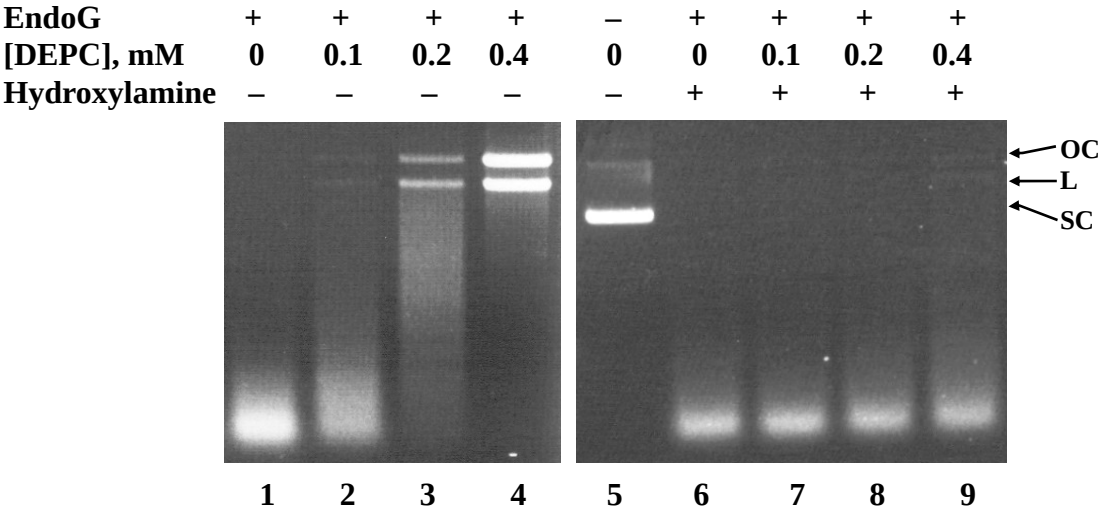

Fig. 3. Chemical modification of human EndoG. EndoG (0.2 pmol) was mixed with various amounts of DPEC and incubated at 25^0C for 30 min. The residual activity was analyzed by standard assay conditions (*lanes 1* to *4*). An assay for restoration with hydroxylamine was performed by incubating 20 mM hydroxylamine and DEPC-treated EndoG together at 4^0C for 5 h. The residual activity was then analyzed (*lanes 6* to *9*). *Lane 5* represents the reaction performed in the absence of EndoG. *Arrowheads* denote the different topological forms of pUC18 plasmids. OC: open circular; L: linear; SC: supercoiled.

(A)

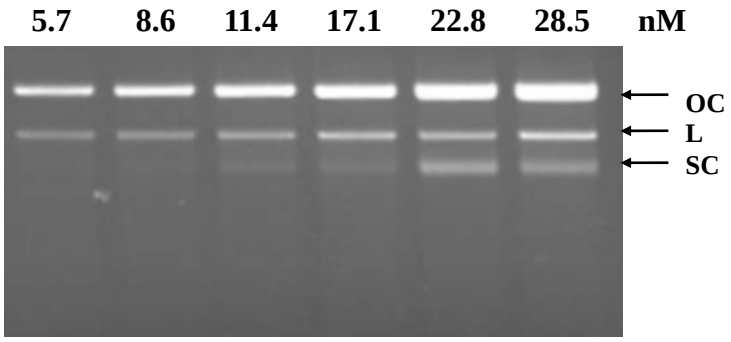

(B)

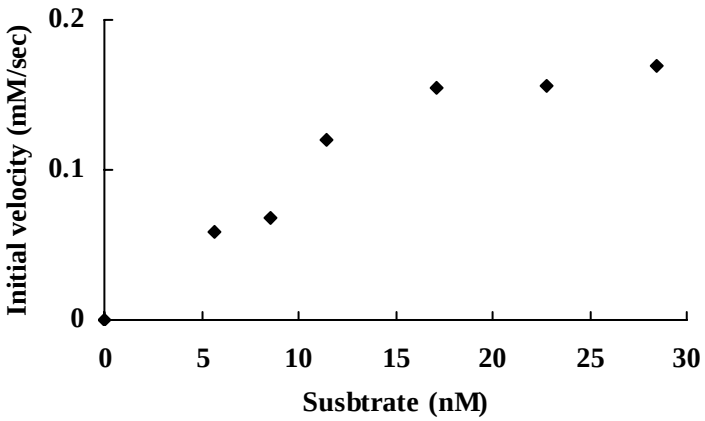

Fig. 4. Kinetic analysis of human EndoG. *A*, Electrophoresis analysis. EndoG (0.05 pmol) was mixed with various amounts of supercoiled pUC18 dsDNA and incubated at 37^0C for 3 min. The resulting products were then analyzed by 1.2% agarose gels. *Arrowheads* denote the different topological forms of pUC18 plasmids. OC: open circular; L: linear; SC: supercoiled. *B*, Initial velocity of DNA cleavage as a function of substrate concentration. Steady-state kinetic parameters were determined by curve fitting of these values to the Michaelis-Menten equation.

(A)

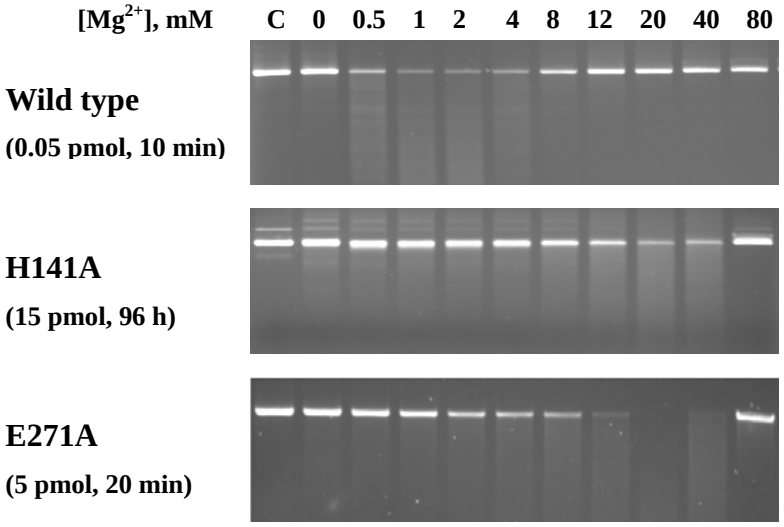

(B)

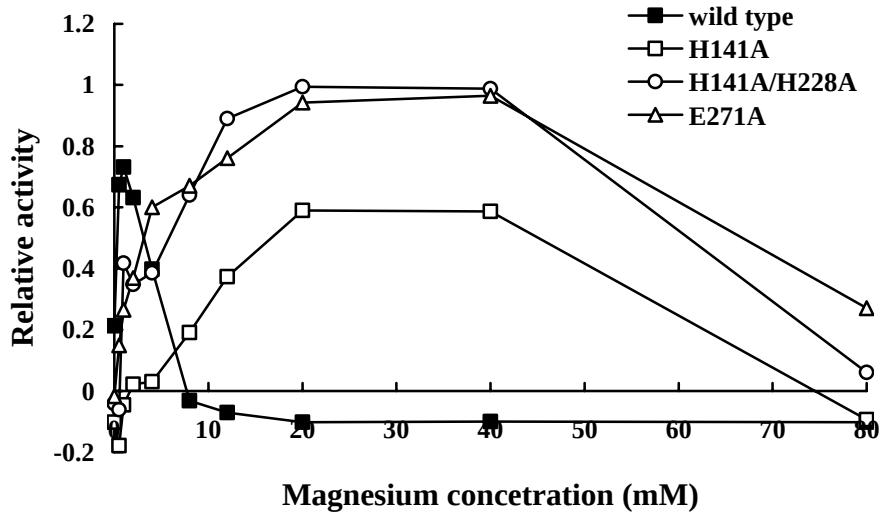

Fig. 5. Magnesium requirements of human EndoG variants. *A*, Electrophoresis analysis. EndoG variants were mixed with 0.1 μg of linear pUC18 dsDNA in EndoG buffer containing various amounts of magnesium. The reaction mixtures were incubated at 37^0C for indicated periods. The resulting products were analyzed by 1.2% agarose gels. *Lane C* represents the reaction performed in the absence of EndoG. *B*, Densitometric analysis. Activities are given as relative values with respect to the maximum activity for each variant.

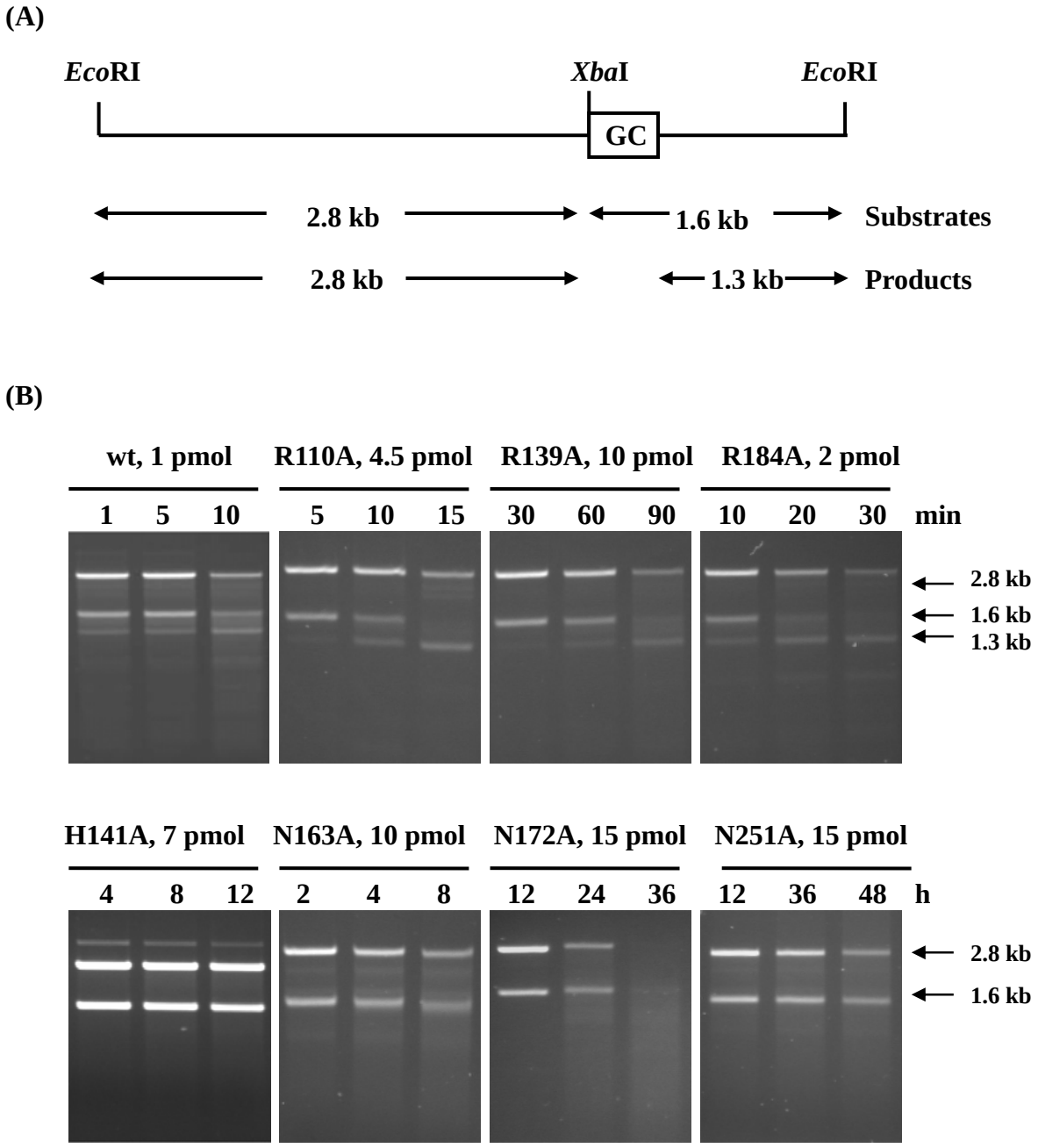

Fig. 6. Cleavage specificities of human EndoG variants. *A*, Sequence-specific cleavage assay. The structure of *Eco*RI-linearized pKJH20 DNA is shown at the top, with the open box designating the GC-rich sequence region (0.3 kb). *Xba*I site is located 1.6 kb from the *Eco*RI site at the 3′ end of the linear pKJH20 DNA. In the cleavage assay, pKJH20 was cleaved by *Eco*RI and *Xba*I to generate the 2.8-kb and 1.6-kb substrates. Enzymes cleaving within the GC-rich sequence are expected to generate both the 2.8-kb and the 1.3-kb product fragments. *B*, Electrophoresis analysis. The reaction mixtures containing 0.2 μg *Eco*RI/*Xba*I-treated pKJH20 and EndoG variants were incubated at 37^0C for various periods. The resulting products were analyzed by 1.2% agarose gels. *Arrowheads* denote the substrate and product fragments.

(A)

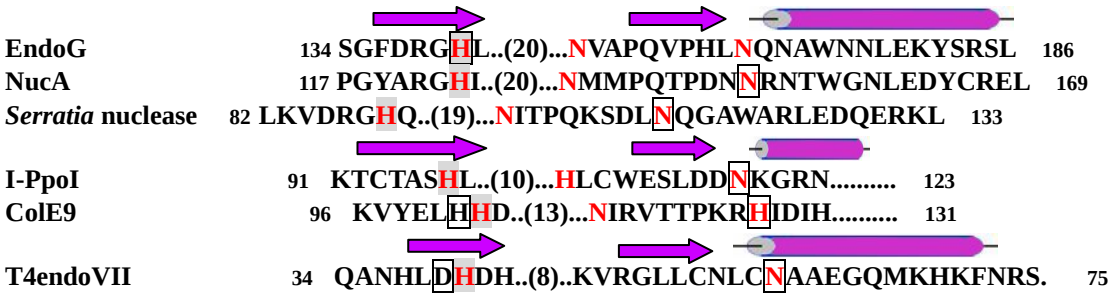

(B)

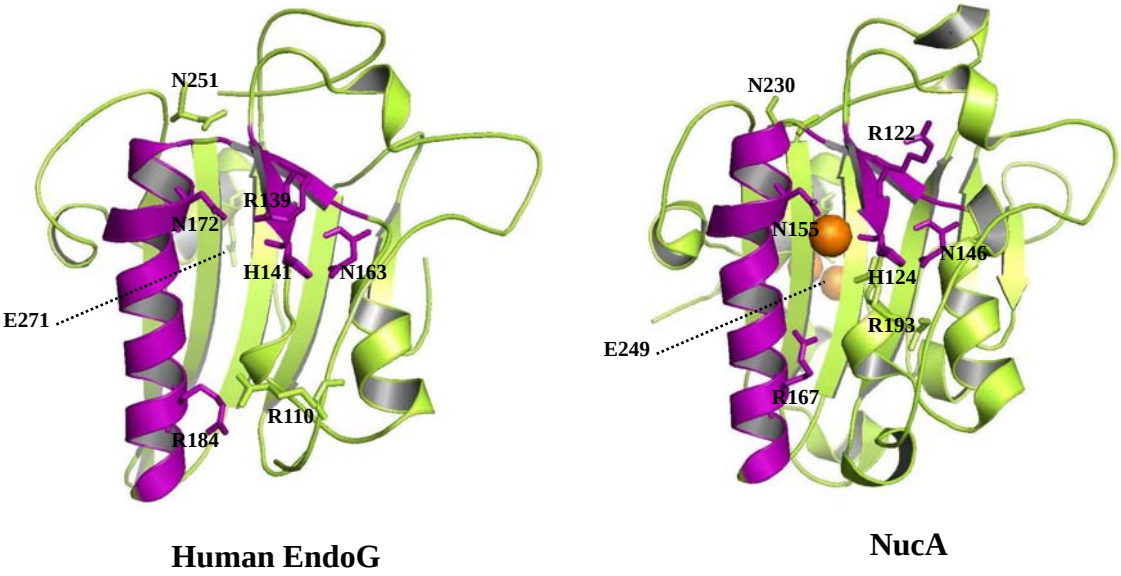

Human EndoG **NucA**

Fig. 7. Sequence alignment and structure of H-N-H nucleases. *A*, Multiple alignment of human EndoG H-N-N motif with H-N-H nucleases. Amino acid sequences of human EndoG (48), NucA (49), *Serratia* nuclease (50), ColE9 (51), I-*Ppo*I (52), and T4endoVII (53) were aligned. The amino acid residues representing the H-N-H motif are highlighted in *red*. The two β-strands and the α-helix of H-N-H motif are indicated by *arrows* and *tube*, respectively. The amino acid residues acting as general bases are highlighted in *grey*. *Boxed residues* represent the amino acid residues involved in magnesium coordination. *B*, Comparison of the modeled structure of human EndoG and the experimentally solved structure of NucA (PDB code 1ZM8). ββα-Me-finger motif is highlighted in *purple*. Amino acid residues involved in catalysis, magnesium coordination, and substrate specificity are indicated and labeled.